assistance of Patrick Ryan in the preparation of the manuscript. Portions of the computational work were performed by use of GAUSSIAN 86 on the NCSA Cray XMP/48 under an affiliate training grant.

Supplementary Material Available: Listing of full Cartesian coordinates and total energies for all optimized structures included in this paper (1 page). Ordering information is given on any current masthead page.

Vibrational Circular Dichroism in Methylthiirane: Ab Initio Localized Molecular Orbital Predictions and Experimental Measurements

P. L. Polavarapu,* P. K. Bose, and S. T. Pickard

Contribution from the Department of Chemistry, Vanderbilt University, Nashville, Tennessee 37235. *Received February 5, 1990*

Abstract: Vibrational circular dichroism (VCD) spectra for both enantiomers of methylthiirane were measured in CCl_4 and CS_2 solutions, and also in the vapor phase. The first ab initio localized molecular orbital (LMO) predictions of vibrational circular dichroism were carried out. The LMO-VCD predictions were found to be in satisfactory agreement with the experimental observations.

1. Introduction

Theoretical models[1,2] for understanding the vibrational circular dichroism (VCD) phenomenon have played a major role in the development of VCD spectroscopy. After the first measurements of VCD by Holzwarth and co-workers[3] and by Nafie, Keiderling, and Stephens[4] several groups[5] have contributed to the theoretical and experimental details. VCD spectroscopy has now come to a stage where excellent quality VCD spectra can be recorded and exact theoretical formulations are available. The implementation of these theoretical formulations, however is plagued by practical problems as described below.

VCD intensity for a given vibrational transition is determined by the product of electric and magnetic dipole transition moments. While the evaluation of electric dipole transition moments, which also determine the vibrational absorption intensities, is very well-known, special care is required in formulating the magnetic dipole transition moment, because the electronic contribution to this transition moment vanishes if one confines the formulation to the uncorrected Born–oppenheimer (BO) wave function (vide infra). Currently there are three distinct approaches to the quantum mechanical evaluation of magnetic dipole transition moments. The first approach referred to as localized molecular orbital (LMO) formulation was due to Walnut and Nafie.[6] In this approach they corrected the BO wave function to incorporate the correlation between nuclear and electronic velocities, which is necessary to retrieve the vanishing electronic contribution to the magnetic dipole transition moments. This initially leads to an expression that involves the summation over all excited electronic states. This sum, however, was reduced to a product of vibronic gauge function and ground electronic wave function. This vibronic gauge function was specified by a differential equation and solved for a set of elliptical and Gaussian orbitals that depend on the nuclear displacements. The rocking motion of these elliptical orbitals can contribute to the magnetic dipole transition moment, and this contribution is difficult to evaluate in general. Nevertheless, it was argued[6] that this contribution represents only 15% (approximately) of the total magnetic dipole transition moment and therefore can be ignored. If the orbitals are spherical, the rocking contributions to the magnetic dipole transition moment are identically zero. In the absence of spherical orbitals, one could localize the molecular orbitals to minimize this rocking contribution.

An alternate, but less rigorous, approach to LMO-VCD formulation was also advanced by Nafie and Walnut,[7] along with the rigorous approach of Walnut and Nafie. A more general account of LMO-VCD approach, along with calculational results, was presented by Nafie and Polavarapu.[8] The calculations reported to date[8,9] employed CNDO wave functions[10] whose quality is not reliable enough to seriously judge the reliability, or otherwise, of LMO-VCD predictions.

An exact quantum mechanical approach, which we refer to as the magnetic field perturbative (MFP) method, for the magnetic dipole transition moment is now well-documented.[11-15] In this MFP approach also one starts with a corrected BO wave function which leads to an expression that involves the summation over excited electronic states. In contrast to the approach of Walnut and Nafie, it was shown that this sum-over excited states expression for magnetic dipole transition moment can be replaced by the overlap of nuclear displacement derivative with the magnetic field derivative of the same ground electronic state wave function.

(1) Deutsche, C. W.; Moscowitz, A. *J. Chem. Phys.* **1968**, *49*, 3257-3272; **1970**, *53*, 2630-2644.
(2) Schellman, J. A. *J. Chem. Phys.* **1973**, *58*, 2882-2886; -1974, *60*, 343.
(3) Holzwarth, G.; Hsu, E. C.; Mosher, H. S.; Faulkner, T. R.; Moscowitz, A. *J. Am. Chem. Soc.* **1974**, *96*, 251-252.
(4) Nafie, L. A.; Keiderling, T. A.; Stephens, P. J. *J. Am. Chem. Soc.* **1976**, *98*, 2715-2723.
(5) For a collection of references on the subject see: Polavarapu, P. L. *Vibrational Spectra and Structure*; Bist, H. D., Durig, J. R., Sullivan, J. F., Eds.; Elsevier: New York, 1989; Vol. 17B, pp 319-342.
(6) Walnut, T. W.; Nafie, L. A. *J. Chem. Phys.* **1977**, *67*, 1501-1510.
(7) Nafie, L. A.; Walnut, T. W. *Chem. Phys. Lett.* **1977**, *49*, 441.
(8) Nafie, L. A.; Polavarapu, P. L. *J. Chem. Phys.* **1981**, *75*, 2935-2944.
(9) Polavarapu, P. L.; Nafie, L. A. *J. Chem. Phys.* **1981**, *75*, 2945-2951. Freedman, T. B.; Diem, M.; Polavarapu, P. L.; Nafie, L. A. *J. Am. Chem. Soc.* **1982**, *104*, 3343-3349. Annamalai, A.; Keiderling, T. A.; Chicos, J. S. *J. Am. Chem. Soc.* **1984**, *106*, 6254-6262. Annamalai, A.; Keiderling, T. A.; Chicos, J. S. *J. Am. Chem. Soc.* **1985**, *107*, 2285-2291. Narayanan, U.; Keiderling, T. A. *J. Am. Chem. Soc.* **1988**, *110*, 4139-4144. Annamalai, A.; Jalkanen, K. J.; Narayanan, U.; Tissot, M. C.; Keiderling, T. A.; Stephens, P. J. *J. Phys. Chem.* **1990**, *94*, 194-199.
(10) Pople, J. A.; Beveridge, D. L. *Approximate Molecular Orbital Theory*; McGraw Hill: New York, 1970.
(11) Galwas, P. A. Ph.D. Thesis, University of Cambridge, Cambridge, UK, 1983.
(12) Buckingham, A. D.; Fowler, P. W.; Galwas, P. A. *Chem. Phys.* **1987**, *112*, 1-14.
(13) Stephens, P. J. *J. Phys. Chem.* **1985**, *89*, 748-752.
(14) Amos, R. D.; Handy, N. C.; Drake, A. F.; Palmieri, P. *J. Chem. Phys.* **1988**, *89*, 7287-7297.
(15) Salzman, W. R. *J. Phys. Chem.* **1989**, *93*, 7351-7354.

0002-7863/91/1513-43$02.50/0

Although this MFP method is exact, the gauge origin dependence of the magnetic field dependent properties (when the wavefunction is not exact) introduces some practical problems. The center of mass (COM) and center of charge (COC) serve as convenient points of reference, but it is not clear that they represent optimal points for VCD calculations. A distributed origin (DO) gauge,[16] much like the local origin analogue of Hansen and Bouman,[17] was shown to give origin-independent VCD results, but again it is not known that the DO gauge is the best choice that there can be for VCD results. For instance, VCD predictions obtained for methylthiirane with DO gauge were considered[18] to be in poorer agreement with the experimental results than they are when obtained with other choices for gauge origin. Unless the wave function is near the Hartree–Fock limit the gauge origin is likely to be an irritating problem for the MFP method as exemplified by methylthiirane.[18]

Note that both the LMO and MFP methods start with the corrected BO wave functions (involving sum-over electronic states expression), but the end result was obtained without involving the sum-over electronic states. The vibronic coupling VCD method due to Nafie and Freedman[19] and implemented by Dutler and Rauk[20] differs from the LMO and MFP approaches by evaluating the sum-over excited electronic states expression explicitly. Dutler and Rauk have used special criteria and a special set of derivatized basis functions to truncate the summation over excited electronic states. Encouraging VCD predictions were obtained for the limited number of molecules investigated thus far. Major practical problems are introduced, however, by the need for, and the size of, the derivatized basis functions. For instance, methylthiirane represents an unwieldy molecule for vibronic coupling VCD calculations (but not so for MFP and LMO methods) at least as of now. In addition, vibronic coupling VCD results[20] as they are obtained now depend on the molecular origin.

The LMO-VCD calculations are quite useful from the viewpoint of chemical insight. That is, this approach provides a pictorial insight on how the bonding (or lone pair) electrons react to the nuclear displacements and are responsible for generating the magnetic dipole transition moments. In order to trust the ensuing chemical picture, the LMO method should be tested first for reliable VCD predictions. Such verification is lacking as LMO-VCD calculations have not been performed with ab initio wave functions. This led us to undertake systematic ab initio LMO-VCD calculations for a variety of chiral molecules for which the experimental data are available. In this paper, we present the ab initio LMO-VCD results for methylthiirane. Although the experimental VCD spectra for methylthiirane were reported previously,[21] we have remeasured these spectra with much improved signal-to-noise ratio using a recently built VCD spectrometer. In addition, we have also recorded the VCD spectra for methylthiirane in the vapor phase, to avoid the possible intermolecular effects in the condensed liquid phase, and to investigate if any unusual effects in the rotational–vibrational transitions, such as those found[22] for methyloxirane, can be seen. These experimental results are also presented in this article.

2. Theoretical and Computational Details

For a fundamental (one quantum) vibrational transition, associated with normal mode Q_l, the circular dichroism intensity is represented by rotational strength R_l, where

$$R_l = \mathrm{Im}\,\langle\psi_{00}|\mu_\alpha|\psi^l_{01}\rangle\langle\psi^l_{01}|\mathrm{m}_\alpha|\psi_{00}\rangle \qquad (1)$$

In eq 1, ψ_{00} is the total wave function for a molecule in the electronic and vibrational ground states; ψ^l_{01} is the wave function in an excited vibrational state belonging to the ground electronic state with superscript l indicating that a single vibrational mode Q_l is excited; μ_α and m_α are the electric and magnetic dipole moment operators, respectively. In the formalism of Walnut and Nafie, eq 1 is reduced to

$$R_l = \frac{e^2h}{8\pi c}[\{\sum_A Z_A S^l_{A\alpha} - \sum_K \sigma^l_{K\alpha}\}\{\sum_A Z_A \epsilon_{\alpha\beta\gamma} R^0_{A\beta} S^l_{A\gamma} - \sum_K \epsilon_{\alpha\beta\gamma} r^0_{K\beta} \sigma^l_{K\gamma} - \sum_K \tau^l_{K\alpha}\}] \qquad (2)$$

In eq 2, Z_A is the bare nuclear charge of atom A, with equilibrium positional coordinates $R^0_{A\beta}$ and normal vibrational displacement $S^l_{A\alpha}$; $r^0_{K\alpha}$ and $\sigma^l_{K\alpha}$ represent respectively the orbital centroid and its normal vibrational displacement of the Kth occupied molecular orbital; $\epsilon_{\alpha\beta\gamma}$ is the alternating tensor; and $\tau^l_{K\alpha}$ represents the rocking contribution of the Kth orbital during the normal vibration Q_l. These rocking contributons are hoped to be small for the localized molecular orbitals and are therefore ignored. This leads to eq 2 being written as[6-8]

$$R_l = \frac{e^2h}{8\pi c}[\{\sum_A Z_A S^l_{A\alpha} - \sum_K \sigma^l_{K\alpha}\}\{\sum_A Z_A \epsilon_{\alpha\beta\gamma} R^0_{A\beta} S^l_{A\gamma} - \sum_K \epsilon_{\alpha\beta\gamma} r^0_{K\beta} \sigma^l_{K\gamma}\}] \qquad (3)$$

which represents the LMO expression for VCD intensity.

The equilibrium nuclear coordinates $R^0_{A\alpha}$ were obtained through geometry optimization with GAUSSIAN 86[23] or CADPAC[24] programs. The nuclear vibrational displacements $S^l_{A\alpha}$ were obtained through the analytic frequency calculations with the same programs. The localized orbital centroids $r^0_{K\alpha}$ were obtained with the GAMESS program[25] employing Boys' localization scheme.[26] The 1s and 2s core orbitals of sulfur were frozen during localization. The vibrational displacements $\sigma^l_{K\alpha}$ of the orbital centroids were obtained numerically, by evaluating the orbital centroids at the nuclear geometries displaced by ±0.005 Å from the equilibrium geometry. For the present calculations, the 6-31G* basis set provided in the program libraries[23-25] was used. This basis set was found to provide satisfactory predictions of vibrational absorption, Raman, and Raman optical activity spectra for methylthiirane.[27,28] As the same basis set was used earlier by Dothe et al.[18] for VCD predictions with the MFP method, a direct comparison of the predictive capabilities of LMO and MFP methods can be made.

3. Experimental Details

The VCD spectra were recorded in the ~1600–650-cm^{-1} region for both enantiomers of methylthiirane in CCl_4 and CS_2 solvents. These measurements were made at 4-cm^{-1} resolution with a VCD spectrometer built around a CYGNUS-100 (Mattson Instruments) FTIR optical bench. The data collection time for each sample was approximately 1 h (6000 scans). Measurements for vapor-phase samples of methylthiirane were obtained at 1-cm^{-1} resolution. For these measurements, a single-pass gas cell with 5-cm path length was used. The data collection time for each sample was approximately 4 h (6000 scans). The absorption spectra of the neat liquid samples are identical with those reported earlier,[21,27] except for the weak band at ~1100 cm^{-1} present for a previous sample.[21] While comparing the present absorption spectra recorded in CCl_4 and CS_2 solutions to the neat liquid spectra, the solvent absorption

(16) Stephens, P. J. *J. Phys. Chem.* **1987**, *91*, 1712–1715. Stephens, P. J.; Jalkanen, K. J.; Amos, R. D.; Lazaretti, P.; Zanasi, R. *J. Phys. Chem.* **1990**, *94*, 1811–1830 and cross references cited therein.
(17) Hansen, A. E.; Bouman, T. D. *J. Chem. Phys.* **1985**, *82*, 5035–5047.
(18) Dothe, H.; Lowe, M. A.; Alper, J. S. *J. Phys. Chem.* **1988**, *92*, 6246–6249.
(19) Nafie, L. A.; Freedman, T. B. *J. Chem. Phys.* **1983**, *78*, 7106–7108.
(20) Dutler, R.; Rauk, A. *J. Am. Chem. Soc.* **1989**, *111*, 6957–6966.
(21) Polavarapu, P. L.; Hess, B. A., Jr.; Schaad, L. J.; Henderson, D. O.; Fontana, L. P.; Smith, H. E.; Nafie, L. A.; Freedman, T. B.; Zuk, W. M. *J. Chem. Phys.* **1987**, *86*, 1140–1146.
(22) Polavarapu, P. L. *Chem. Phys. Lett.* **1989**, *161*, 485–490.
(23) Frisch, M. J.; Binkley, J. S.; Schlegel, H. B.; Raghavachari, K.; Melius, C. F.; Martin, R. L.; Stewart, J. J. P.; Bobrowicz, F. W.; Rohlfing, C. M.; Kahn, L. F.; Defrees, D. J.; Seeger, R.; Whiteside, R. A.; Fox, D. J.; Fluder, E. M.; Pople, J. A. GAUSSIAN 86; Carnegie Mellon Quantum Chemistry Publishing Unit: Pittsburgh, 1984.
(24) Amos, R. D.; Rice, J. E. CADPAC: The Cambridge Analytic Derivative Package, Issue 4.0, Cambridge, 1987.
(25) Schmidt, M. W.; Boatz, J. A.; Baldridge, K. K.; Koseki, S.; Gordon, M. S.; Eldbert, S. T.; Lam, B. *QCPE Bull.* **1987**, *7*, 115. Dupius, M.; Spangler, D.; Wendoloski, J. J. NRCC Program QG01; University of California, Berkeley, CA, 1980.
(26) Foster, J. M.; Boys, S. F. *Rev. Modern. Phys.* **1960**, *32*, 300–302.
(27) Bose, P. K.; Polavarapu, P. L. *Chem. Phys. Lett.* **1988**, *152*, 39–43. Polavarapu, P. L. *Ibid.* **1990**, *163*, 576–580.
(28) Bose, P. K.; Barron, L. D.; Polavarapu, P. L. *Chem. Phys. Lett.* **1989**, *155*, 423–429.

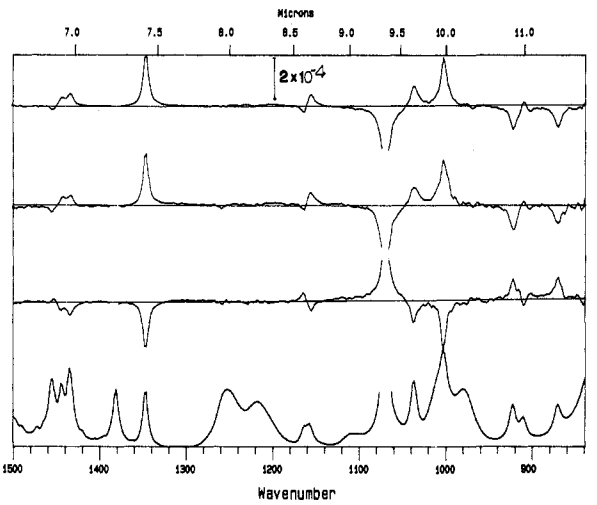

Figure 1. Vibrational absorption (bottom) and VCD spectra for methylthiirane in CCl_4 solution (0.7 M) at 4-cm^{-1} resolution. The path length employed was approximately 475 μm. The top-most VCD spectrum is obtained by taking one-half of the difference between the raw VCD spectra of (+) and (−) enantiomers. The next two are obtained by subtracting the raw VCD spectrum of the racemic mixture from that of (+) and (−) enantiomers respectively. The data collection time is ~1 h per sample. The absorption spectrum is plotted on the 0–0.9 absorbance scale. Due to excessive absorbance, the band at 1070 cm^{-1} is not shown fully. Note that the solvent has absorption bands at ~979, 1005, 1067, 1110, 1218, and 1252 cm^{-1}.

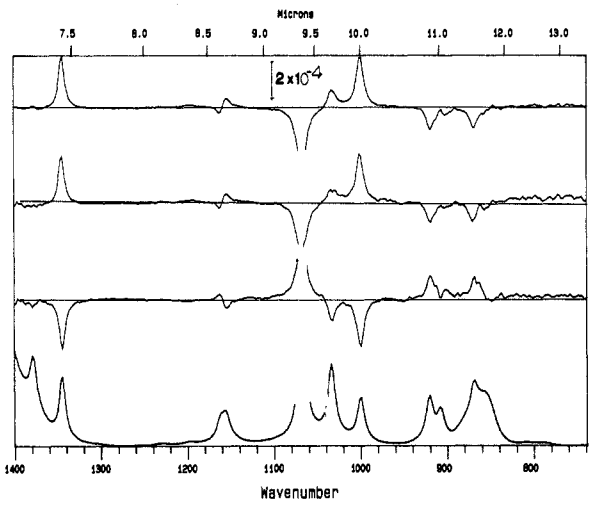

Figure 2. Vibrational absorption (bottom) and VCD spectra for methylthiirane in CS_2 solution (0.7 M) at 4-cm^{-1} resolution. The path length employed was approximately 600 μm. The top-most VCD spectrum is obtained by taking one-half of the difference between the raw VCD spectra of (+) and (−) enantiomers. The next two are obtained by subtracting the raw VCD spectrum of the racemic mixture from that of (+) and (−) enantiomers, respectively. The data collection time is ~1 h per sample. The absorption spectrum is plotted on the 0–0.9 absorbance scale. Due to excessive absorbance, the band at 1070 cm^{-1} is not shown fully. Note that the solvent has an absorption band at ~856 cm^{-1}.

bands should be taken into consideration.

The integrated absorption intensities of individual bands were obtained through curve fitting with use of the software supplied by Mattson Instruments, Inc. Rotational strengths were determined by integrating the VCD band envelopes and dividing by the wavenumber at the band center. In cases where the VCD bands strongly overlap, the combined value is reported. Due to the uncertainties in the measurement of the path length of the cells or the vapor pressure used, the relative intensities are presented.

The (*R*) and (*S*) enantiomers of methylthiirane, prepared as described elsewhere,[21] had optical rotations respectively of $[\alpha]^{25}_D$ +24.1° and −20.6° (neat, 0.5 dm). The proton NMR spectra are identical with those reported earlier.[21] The racemic form of methylthiirane was purchased from Aldrich Chemical Co.

4. Results and Discussion

The experimental VCD spectra, in the ~1500–800-cm^{-1} region, for both enantiomers of methylthiirane in CCl_4 and CS_2 solutions are shown in Figures 1 and 2. The absorption band at ~1380 cm^{-1}, which was assigned[21] to the symmetric methyl bending mode, does not have significant VCD. The absorption band at ~911 cm^{-1} also does not exhibit significant VCD in CS_2 solution, but it shows a small VCD feature in CCl_4 solution (positive for the (*R*) enantiomer). The larger negative VCD feature associated with the neighboring band at ~922 cm^{-1} appears to be reducing the magnitude of the small positive VCD associated with the ~911-cm^{-1} band.

The vapor-phase VCD measurements, showing rotational-vibrational features and hence referred to as rotational–vibrational circular dichroism (RVCD), at 1- and 4-cm^{-1} resolutions are shown in Figure 3. Although the individual rotational–vibrational transitions are not resolved, the P, Q, R envelopes can be clearly seen. The close spacing of some vibrational bands and larger band spreads in the vapor-phase spectra cause the associated bisignate CD features (which could be clearly seen in the condensed liquid phase VCD spectra) to mutually cancel and therefore are not apparent in the RVCD spectra. For example the bisignate VCD feature present at ~1160 cm^{-1} for the liquid-phase sample (see Figures 1 and 2) is not present for the vapor-phase sample (Figure 3). From this viewpoint, RVCD spectra are not any more helpful than the VCD spectra. However, one important feature of RVCD spectra is that the RVCD associated with the Q envelope does not have to be of the same sign as that associated with the P and R envelopes. In favorable cases the relative magnitudes of the

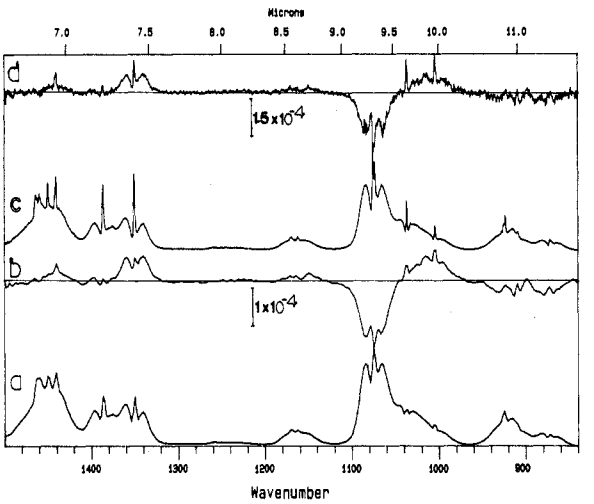

Figure 3. Vibrational absorption (a, c) and rotational–vibrational CD (RVCD) spectra (b, d) of (*R*)-(+)-methylthiirane in the vapor phase at 4-cm^{-1} resolution (a, b) and 1-cm^{-1} resolution (c, d). RVCD spectra were obtained by taking one-half of the difference between the RVCD spectra of (+) and (−) enantiomers. The data collection time for 1 cm^{-1} resolution RVCD spectra is approximately 4 h per sample. The absorption spectra are plotted on 0 to 0.6 (a) and 0 to 0.8 (c) absorbance scales.

individual components of rotational strength can be deduced from the RVCD spectra through simulation as was done by Salzman.[29] For methyloxirane, we found[22] that RVCD associated with the Q branch is opposite to that of P and R branches, which results from the fact that the three components, which comprise rotational strength, need not all have the same sign. Such sign reversals are not evident for any of the isolated bands of methylthiirane.

In the experimental region of 1500–800 cm^{-1}, there are 13 vibrational bands with band centers at 1454, 1443, 1434, 1380, 1347, 1162, 1158, 1070, 1038, 1001, 922, 911, and 870 cm^{-1}. The vibrational band assignments based on the 6-31G* theoretical predictions were discussed earlier[28] in connection with Raman and Raman optical activity. These experimental bands correspond to the 6-31G* theoretical modes with frequencies of 1644, 1640,

(29) Salzman, W. R. Personal communication.

Table I. Vibrational Absorption and Circular Dichrosim Intensities for (*R*)-Methylthiirane

experimental[a]					LMO Calculations[b]						literature calculations[18] roational-strength			
		relative intensities			unscaled			scaled						
freq, cm^{-1}			rotational strength		freq,	IR	rotational	freq,	IR	rotational	freq,			
liquid	vapor	absorption	liquid	vapor	cm^{-1}	intensity	strength	cm^{-1}	intensity	strength	cm^{-1}	DOG[c]	COM[c]	sulfur[c]
1454 (1451)	1461	0.7	−0.04		1644	4.6 (0.6)	5.2 (0.3)	1470	3.9	5.4	1452	−8.3	−3.5	−8.0
1443 (1443)	1450	0.7		+0.3	1640	6.3 (0.8)	1.0 (0.1)	1461	6.3	2.2	1446	3.2	−5.4	12.2
			+0.4											
1434 (1433)	1441	1.1			1628	3.6 (0.5)	5.3 (0.3)	1450	4.3	5.8	1434	5.5	17.7	31.5
1380 (1378)	1386	0.7	*d*	*d*	1572	1.9 (0.3)	−1.9 (−0.1)	1394	1.9	−3.0	1387	3.8	0.85	7.2
1347 (1346)	1350	1.0	+1.0	+1.0	1519	7.5 (1.0)	17.8 (1.0)	1355	4.7	5.2	1341	4.7	15.0	−38.2
1162 (1162)	1162				1305	3.4 (0.5)	−7.8 (−0.4)	1188	10.2	28.1	1169	5.3	35.9	37.6
		0.6	+0.1	+0.3										
1158 (1153)					1285	8.3 (1.1)	15.9 (0.9)	1162	2.1	−5.0	1151	−0.54	5.2	−5.3
1070 (1066)	1074	1.7	−2.0[e]	−3.2	1223	26.2 (3.5)	−35.4 (−2.0)	1085	26.6	−39.7	1078	−6.1	−173.7	−187.5
1038 (1034)	1036	0.7	+0.5		1183	7.6 (1.0)	0.7 (0.0)	1049	9.5	2.8	1043	−1.5	40.9	33.2
				+1.6										
1001 (1001)	1003	0.7	+1.4		1126	2.5 (0.3)	4.2 (0.2)	998	2.8	4.4	992	10.1	73.2	77.2
922 (922)	924	0.7			1032	2.6 (0.3)	−12.7 (−0.7)	915	2.9	−15.2	908	−0.07	−21.6	−21.9
			−0.7	−0.7										
911 (909)		0.4			1010	2.4 (0.3)	9.6 (0.5)	903	2.4	20.5	896	6.6	54.2	52.7
870 (870)	870	0.5	−0.6	−0.8	954	1.6 (0.2)	−5.0 (−0.3)	868	1.8	−13.9	861	−6.7	−36.8	−22.5
					707	5.3 (0.7)	9.6 (0.5)	642	7.8	10.1	628	3.3	22.1	30.2
					660	46.1 (6.1)	−12.9 (−0.7)	601	42.5	−14.5	585	−4.4	−14.4	−18.4
					413	0.2 (0.0)	1.5 (0.1)	380	0.2	2.0	377	0.95	−1.7	−5.9
					328	1.6 (0.2)	−0.7 (−0.0)	302	1.7	−0.5	301	−3.9	−0.82	1.5
					245	0.1 (0.0)	0.9 (0.1)	220	0.1	0.8	220	3.7	7.9	7.1

[a] The listed band centers were determined by peak-picking software; those obtained in the curve-fitting procedure with use of the first derivative spectrum are given in parentheses. Absorption intensities for the neat liquid were determined by using curve-fitting software. Rotational strengths were obtained from the frequency weighted integrated areas of the VCD bands with use of the 4-cm^{-1} resolution spectra. For the liquid phase these were obtained from the spectra in CCl_4 (1500–1350 cm^{-1}) and CS_2 (1350–700 cm^{-1}) solutions. [b] Calculations were done with the 6-31G* basis set, at the optimized geometries. IR intensities are given in km/mol. Rotational strength, R_l, is given in 10^{-44} esu^2 cm^2. Relative intensities are given in parentheses. [c] DOG, COM, and sulfur represent respectively the distributed origin gauge, the gauge origin at the center of mass, and the gauge origin at sulfur. [d] Weak. [e] This value is not definitive due to excessive absorbance at this band.

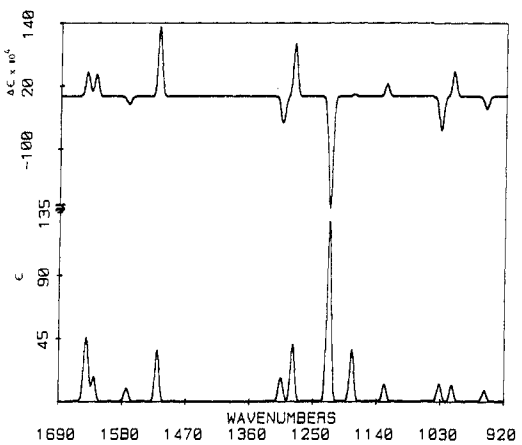

Figure 4. Vibrational absorption (bottom) and LMO-VCD (top) predicted for (*R*)-methylthiirane with the 6-31G* basis set and plotted as ϵ and $\Delta\epsilon$ in L/(mol cm). These were simulated from the absorption intensities and rotational strength (Table I) by using Gaussian intensity distribution and a 5 cm^{-1} half-width at $1/e$ of the peak height.

1628, 1572, 1519, 1305, 1285, 1223, 1183, 1126, 1032, 1010, and 954 cm^{-1}, respectively (see Figure 4, Table I). The infrared absorption, Raman, and Raman optical activity (ROA) spectral predictions obtained with the 6-31G* basis were already discussed and were found[27,28] to be in pleasing agreement with the corresponding experimental observations. Therefore, the discussion on vibrational analysis is not repeated here. The LMO–VCD intensities are summarized in Table I, and the simulated spectrum is shown in Figure 4. We have also carried out calculations using the scaled 6-31G* force constants, with the same scale factors that were used[18] in the MFP calculations. The resulting frequencies and intensities are also summarized in Table I. The frequencies resulting from the scaled calculation are slightly different from those of Dothe et al.[18] due to the corrected theoretical geometry used in their calculations.

A comparison of Figures 1–3 with Figure 4 reveals that, although there are quantitative differences in intensities (Table I), except for the first higher frequency band the predicted LMO-VCD spectrum resembles the experimental VCD spectrum satisfactorily. A detailed discussion for (*R*)-(+)-methylthiirane is given below.

The first three experimental absorption bands at 1454, 1443, and 1434 cm^{-1} have negative, positive, and positive VCD signs, respectively. The corresponding 6-31G* theoretical modes at 1644, 1640, and 1628 cm^{-1} have all positive VCD signs, with the first one at variance with the experimental observation as mentioned above. The MFP calculation,[18] with distributed origin gauge, predicts correct sign order for these three bands, but the predicted relative magnitude for the first one is much larger than that observed. The MFP calculation[18] with gauge origin at the center of mass of the molecule predicts the wrong sign for the second one of these three bands while that with the gauge origin at sulfur correctly predicts the sign pattern.

For the next experimental band at 1380 cm^{-1}, we could not obtain measurable VCD, which is supported by the LMO-VCD predictions that the corresponding theoretical mode at 1572 cm^{-1} exhibits only weak VCD. The MFP calculations[18] with distributed origin gauge and with gauge origin at sulfur incorrectly predict a very large magnitude for this band. These same MFP calculations with the gauge origin at the center of mass of the molecule predict small VCD magnitude for this band.

The experimental VCD band at 1347 cm^{-1} and the corresponding LMO-VCD band at 1519 cm^{-1} have positive sign with substantially larger magnitude than the ones discussed in previous paragraphs. Note that the predicted VCD magnitude is lowered by more than three times in the scaled calculation, with a scaled frequency of 1355 cm^{-1}, which compares poorly with the experimental relative VCD magnitudes. The MFP calculations[18] with the gauge origin at the sulfur atom predict the wrong sign for this band.

There are two overlapping experimental bands at 1162 and 1158 cm^{-1} with negative and positive VCD, respectively. This pattern is correctly reproduced in the LMO-VCD calculations for the two corresponding theoretical modes at 1305 and 1285 cm^{-1}. All three MFP calculations[18] incorrectly predict this sign pattern. However, the wrong sign pattern predicted by the MFP calculations with distributed origin gauge and gauge origin at the sulfur atom is

Table II. Vibrational Data[a] for C–H Stretching Modes of Methylthiirane

	unscaled					scaled					literature calculations[18]				experimental[21]		
		IR	Raman				IR	Raman				R_1			freq, cm^{-1}		VCD
assignment	freq, cm^{-1}	intensity, km/mol	$45\alpha_j^2 + 7\beta_j^2$	ρ	R_1	freq, cm^{-1}	intensity, km/mol	$45\alpha_j^2 + 7\beta_j^2$	ρ	R_1	freq, cm^{-1}	DOG	COM	sulfur	Raman	IR	sign
asym CH_2	3407	6.5	72.0	0.71	−2.1	3117	6.5	72.1	0.71	−2.1	3098	−1.6	3.2	−1.7	3057	3060	?
C*–H	3345	17.1	88.5	0.24	2.1	3060	17.0	90.1	0.23	2.6	3040	5.2	−10.5	−10.5	3006	3004	+
sym CH_2	3319	18.2	94.1	0.12	−3.6	3037	18.2	92.4	0.12	−4.0	3018	0.0	3.6	10.4	2987	2981	+
asym CH_3	3292	18.0	67.6	0.75	−3.6	3012	18.0	67.7	0.75	−3.7	2943	−6.4	9.4	21.8		2974	
asym CH_3	3269	23.7	84.8	0.70	8.0	2990	23.7	84.7	0.70	8.0	2919	6.7	−2.0	−9.2	2961	2958	−
sym CH_3	3203	38.0	130.3	0.07	−4.2	2931	38.0	130.4	0.07	−4.2	2861	−0.36	0.59	−3.9	2924	2920	−

[a] Raman intensity parameters are in A^4/amu; $\bar{\alpha}_j$ represents the mean of the polarizability derivative tensor, for the jth vibrational mode, and β_j^2 represents the anisotropy of that tensor. The depolarization ratio ρ is given as $3\beta_j^2/(45\bar{\alpha}_j^2 + 4\beta_j^2)$. Rotational strength parameter R_1 is given in 10^{-44} esu^2 cm^2. For correlation between theoretical modes and experimental bands see the discussion in the text. The present calculations were done with the 6-31G* basis set at the optimized geometry. For scaled calculations, the scale factors from ref 18 were used.

an artifact resulting from the scaling method used in those calculations.[18] As can be seen from the present LMO-VCD calculations (see Table I) with the same scale factors as were used in MFP calculations, the sign pattern is reversed because of the incorrect relative frequency ordering for the two scaled modes at 1188 and 1162 cm^{-1}. As we pointed earlier,[27] the scaling method is susceptible to yielding such misleading results.

The next experimental band at 1070 cm^{-1} has negative VCD and its magnitude is the largest in the 1500–800-cm^{-1} region (see Figure 3). The present LMO-VCD calculations predict the same features for the corresponding theoretical mode at 1223 cm^{-1}. All three MFP calculations[18] also predict the correct sign, but the one with distributed origin gauge predicts the wrong relative magnitude.

The two experimental bands at 1038 and 1001 cm^{-1} have positive VCD with the former VCD band being less intense than the latter. The same features are predicted for the two corresponding theoretical modes, at 1183 and 1126 cm^{-1}, by the present LMO-VCD calculations. The MFP calculation[18] with distributed origin gauge predicts the wrong VCD sign for the first one of these two. The remaining two MFP calculations predict the correct sign pattern.

In the experimental spectrum, the last three bands at 922, 911, and 870 cm^{-1} have negative, very weak (possibly positive), and negative VCD, respectively. The corresponding three theoretical modes at 1032, 1010, and 954 cm^{-1} are predicted by the LMO-VCD calculations to have negative, positive, and negative VCD signs, respectively. The magnitude predicted for the 1010-cm^{-1} theoretical mode is larger than that observed in the experimental spectrum, which is also the case in all MFP calculations.[18] A comparison of unscaled and scaled LMO-VCD results in Table I reveals that scaling method makes the situation worse by nearly doubling the predicted VCD magnitude for this band. The MFP calculation with distributed origin gauge is of poorest accuracy, as negligible VCD was predicted for the first one of these three bands contradicting the experimental observation.

In the C–H stretching region the vibrational band assignments were suggested earlier[21] by comparing the theoretical infrared intensities with the experimental ones using the 6-31G basis set. As the theoretical Raman intensities are also obtained now, we combine the infrared, Raman, and VCD data obtained with the 6-31G* basis set to arrive at plausible assignments. This is summarized in Table II. The experimental Raman bands of methylthiirane at 3057, 3006, 2987, 2961, and 2924 cm^{-1} were suggested[21] to be associated with the antisymmetric CH_2 stretching mode, the C*–H stretching mode, the symmetric CH_2 stretching mode, an antisymmetric CH_3 stretching mode, and the symmetric CH_3 stretching mode, respectively. It was not clear if the remaining antisymmetric CH_3 stretching mode is submerged under the symmetric CH_2 stretching mode or is simply unresolved from the other antisymmetric CH_3 stretching mode. In the experimental polarized Raman spectrum (see Figure 5) the 2987-cm^{-1} band is more intense than the symmetric CH_3 stretching band at 2924 cm^{-1}. The ab initio Raman spectra (Figure 5) obtained with the 6-31G* and 6-31G** basis sets would concur with this experimental observation if the symmetric CH_2 stretching band and one of the two antisymmetric CH_3 stretching modes are closer or

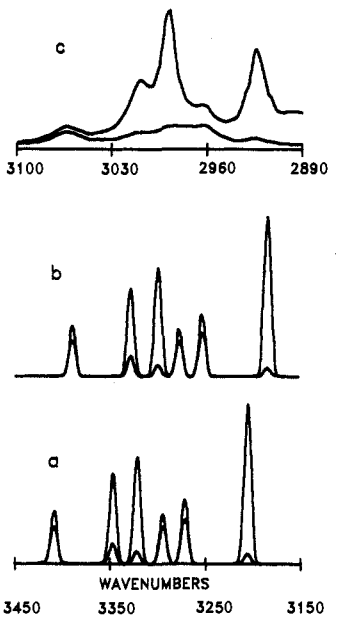

Figure 5. Ab initio (a, b) and experimental (c) Raman spectra for methylthiirane in the C–H stretching region. The ab initio spectra were obtained with 6-31G* (a) and 6-31G** (b) basis sets. The two traces presented in each case represent polarized and depolarized spectra in the 90° scattering geometry.

coincide in their vibrational frequencies. In that case, the simulated LMO-VCD spectra would resemble the experimental VCD spectra, if the lower frequency component of the theoretical antisymmetric CH_3 stretching modes is moved closer to the symmetric CH_2 stretching mode. In other words if the VCD associated with the experimental bands at 2981 and 2974 cm^{-1} is assumed to correspond to the net VCD sum of the ab initio modes at 3319 and 3269 cm^{-1} and that associated with experimental band at 2958 cm^{-1} is assumed to correspond to the VCD of the ab initio mode at 3292 cm^{-1}, then the predicted LMO-VCD sign pattern would be similar to the observed one. Similar agreement would be obtained for the MFP calculations[18] with the distributed origin gauge.

Therefore the main problem in the C–H stretching region lies in the separation of 6-31G* (or 6-31G**) theoretical modes; some of them are separated by a larger frequency gap than the corresponding experimental bands. The literature scaling factors[18] used to bring the theoretical frequencies closer to the experimental ones are not much help, as one can infer from the scaled theoretical frequencies in Table II.

From the above discussion it appears that the VCD predictions obtained with the LMO method are in qualitatively good agreement with the experimental observations in the ~1500–800-cm^{-1} region. The MFP results obtained with the same 6-31G* basis set show notable deviations from the experimental observations. As the vibrational absorption, Raman, and Raman optical activity spectra obtained with the 6-31G* basis set were in satisfactory agreement[27,28] with the corresponding experimental

observations, it is very likely that the failure of MFP method is gauge origin related.

The analysis of the computational time demanded by the analytic LMO and MFP methods would be in favor of the former method. In both methods, the Cartesian derivatives of the electric dipole moment (hence infrared intensities) are obtained in the same manner by using the analytic derivative methods. For obtaining the Cartesian derivatives of the magnetic dipole moment in the LMO method, all the needed parameters are already present in the calculation of the derivatives of the electric dipole moment, except that the expressions have to be recast in terms of the localized molecular orbital centroids. Since the conversion of canonical orbitals to localized orbitals requires only a trivial amount of computer time, the analytic LMO-VCD method (when successfully implemented) would require about the same time as that now required for the vibrational absorption intensities. In the MFP method, the magnetic dipole moment derivatives are obtained by solving the coupled Hartree-Fock (CHF) equations for magnetic field perturbation. In the DO gauge approximation the gauge origin has to be distributed among the N nuclei in the molecule and therefore the CHF equations for the magnetic field perturbation have to be solved N times. Thus the difference in the CPU time required for the MFP and LMO methods is the time required for the N CHF solutions of magnetic field perturbation versus that for localizing the orbitals once.

However, the important consideration is the reliability of predictions offered by a given theoretical method. This can only be determined when more calculations become available. For the LMO method, we have now completed the analysis of results[30-32] for *trans*-oxirane-*2,3-d*$_2$, *trans*-cyclopropane-*1,2-d*$_2$, methyloxirane, *trans*-2,3-dimethyloxirane, *trans*-2,3-dimethylthiirane, and methylcyclopentanone. In all these cases the agreement between the LMO-VCD predictions and the experimental observations is satisfactory.

Besides verifying the theoretical predictions against the experimental VCD observations, there is another way of assessing the predictive capabilities of a given VCD theory. Since the magnetic dipole moment derivatives are related[12] to the paramagnetic magnetizability, one can independently verify the VCD theories using the observed paramagnetic magnetizability. We have also done this comparison[33] for the paramagnetic magnetizability of oxirane, and the LMO predictions compared satisfactorily with the experimental data as well as with that obtained by the MFP method.[34]

5. Summary

Methylthiirane represents a challenging molecule for the theoretical VCD predictions. This is because the exact MFP method was unable to reproduce the experimetal spectrum satisfactorily due to the gauge related problems. The vibronic coupling VCD calculations are, at present, not feasible for methylthiirane, due to the need to augment a chosen basis set with the derivatized basis functions.

We have demonstrated that the ab initio LMO-VCD calculations are feasible and are in good agreement with the experimental observations for methylthiirane. A comparison of unscaled and scaled LMO-VCD predictions with the experimental results indicates that while VCD predictions obtained in the unscaled calculation are in satisfactory agreement with the experimental observations the literature scale factors[18] lead to incorrect frequency ordering for one pair of bands and to incorrect relative VCD magnitudes for some bands. This confirms our earlier conclusion[27] that the scaling method need not give better results than the purely ab initio results.

Although the normal mode displacements of orbital centroids were obtained numerically in the present calculations, they can be obtained by modifying the existing analytic methods for infrared intensities. We are currently planning to implement these analytic methods for VCD calculations, which would make the ab initio LMO-VCD predictions much more routine.

Acknowledgment. We thank Dr. C. S. Ewig and Mr. P. Chan for implementing the GAMESS series of programs. We also thank Professor H. E. Smith for help in the synthesis of optically active methylthiirane samples. This work was supported by grants from NIH (GM29375), NSF (CHE8808018), and Vanderbilt University.

(30) Polavarapu, P. L.; Bose, P. K. *J. Chem. Phys.* In press.
(31) Polavarapu, P. L.; Bose, P. K. *J. Phys. Chem.* In press.
(32) Polavarapu, P. L.; Bose, P. K. Black, T. M. In preparation.
(33) Polavarapu, P. L. *Chem. Phys. Lett.* **1990**, *171*, 271-276.
(34) Stephens, P. J.; Jalkanen, K. J.; Lazzaretti, P.; Zanasi, R. *Chem. Phys. Lett.* **1989**, *156*, 509-519.

Experimental Evidence for the Existence of Polycarbon Oxide Sulfides O(C_n)S (n = 3-5) in the Gas Phase†

Detlev Sülzle and Helmut Schwarz*

Contribution from the Institut für Organische Chemie der Technischen Universität Berlin, D-1000 Berlin 12, Germany. *Received June 4, 1990. Revised Manuscript Received August 3, 1990*

Abstract: The elusive polycarbon oxide sulfides O(C_n)S (n = 3-5) can readily be generated and structurally characterized in the gas phase by electron transfer reactions with use of neutralization-reionization mass spectrometry (NRMS). In addition, for n = 3, 5 both the radical anions and the radical cations are found to exist as stable species having the cumulene connectivity O(C_n)$S^{\bullet-/\bullet+}$. Similarly, the radical cation O(C_4)$S^{\bullet+}$ was structurally characterized as a cumulene. Common to all these species is a straightforward fragmentation pattern that allows an unambiguous structural assignment.

The recent interest[1] in linear and/or quasilinear molecules of the general structure X(C_n)Y (X, Y = lone electron pair, H_2, O, S; $n \geq 2$) containing polycumulated double bonds is due to several factors. These species possess and/or are predicted to exhibit unique spectroscopic and chemical properties; in addition, their reactivity/stability properties as well as their electronic ground state (singlet versus triplet) follow an "odd/even" pattern. In fact, for the *odd*-numbered analogues of X(C_n)Y (n = 3, 5) many

† Dedicated to Professor Dr. Brigitte Sarry on the occasion of her 70th birthday.

(1) For an exhaustive literature coverage, see: Sülzle, D.; Beye, N.; Fanghänel, E.; Schwarz, H. *Chem. Ber.* **1990**, *123*, 2069.

0002-7863/91/1513-48$02.50/0